A Mobility-Resilient Spectrum Sharing Framework for Operating Wireless UAVs in the 6 GHz Band

Jiangqi Hu, *Graduate Student Member, IEEE*, Sabarish Krishna Moorthy, *Student Member, IEEE*, Ankush Harindranath, *Student Member, IEEE*, Zhaoxi Zhang, Zhiyuan Zhao, Nicholas Mastronarde, *Senior Member, IEEE*, Elizabeth Serena Bentley, *Member, IEEE*, Scott Pudlewski, *Senior Member, IEEE*, and Zhangyu Guan, *Senior Member, IEEE*

***Abstract*— To mitigate the long-term spectrum crunch problem, the FCC recently opened up the 6 GHz frequency band for unlicensed use. However, the existing spectrum sharing strategies cannot support the operation of access points in moving vehicles such as cars and UAVs. This is primarily because of the directionality-based spectrum sharing among the incumbent systems in this band and the high mobility of the moving vehicles, which together make it challenging to control the cross-system interference. In this paper, we propose *SwarmShare*, a mobility-resilient spectrum sharing framework for swarm UAV networking in the 6 GHz band. We first present a mathematical formulation of the *SwarmShare* problem, where the objective is to maximize the spectral efficiency of the UAV network by jointly controlling the flight and transmission power of the UAVs and their association with the ground users, under the interference constraints of the incumbent system. We find that there are no closed-form mathematical models that can be used to characterize the statistical behaviors of the aggregate interference from the UAVs to the incumbent system. Then we propose a data-driven three-phase spectrum sharing approach, including *Initial Power Enforcement*, *Offline-dataset Guided Online Power Adaptation*, and *Reinforcement Learning-based UAV Optimization*. We validate the effectiveness of *SwarmShare* through an extensive simulation campaign. Results indicate that, based on *SwarmShare*, the aggregate interference from the UAVs to the incumbent system can be effectively kept below the target level *without* requiring the real-time cross-system channel state information. The mobility resilience of *SwarmShare* is also validated in coexisting networks with *no* precise UAV location information.**

***Index Terms*— Spectrum sharing, swarm UAVs, 6 GHz.**

Manuscript received 23 February 2022; revised 31 December 2022, 17 February 2023, and 23 March 2023; accepted 21 April 2023; approved by IEEE/ACM TRANSACTIONS ON NETWORKING Editor Y. Chen. This work was supported in part by the United States Air Force under Contract FA8750-20-C-1021 and Contract FA8750-21-F-1012 and in part by NSF under Grant SWIFT-2229563. A preliminary shorter version of this paper appeared in the Proceedings of the IEEE International Conference on Sensing, Communication and Networking (SECON), Virtual Conference, July 2021 [DOI: 10.1109/SECON52354.2021.9491602]. *(Corresponding author: Jiangqi Hu.)*

Jiangqi Hu, Sabarish Krishna Moorthy, Ankush Harindranath, Zhaoxi Zhang, Zhiyuan Zhao, Nicholas Mastronarde, and Zhangyu Guan are with the Department of Electrical Engineering, The State University of New York at Buffalo, Buffalo, NY 14260 USA (e-mail: jiangqih@buffalo.edu; sk382@buffalo.edu; ankushha@buffalo.edu; zhaoxizh@buffalo.edu; zzhao24@buffalo.edu; nmastron@buffalo.edu guan@buffalo.edu;).

Elizabeth Serena Bentley is with the Air Force Research Laboratory (AFRL), Rome, NY 13440 USA (e-mail: elizabeth.bentley.3@us.af.mil).

Scott Pudlewski is with the Georgia Tech Research Institute (GTRI), Atlanta, GA 30332 USA (e-mail: scott.pudlewski@gtri.gatech.edu).

Digital Object Identifier 10.1109/TNET.2023.3274354

I. INTRODUCTION

UNMANNED aerial vehicles (UAVs) have been envisioned as a key technology for next-generation (i.e., B5G or 6G) wireless networks [2], [3]. Because of their features of fast deployment, high mobility and small size, UAVs have a great potential to enable a wide set of new applications, including UAV-aided guidance [4], small cells with flying base stations [5], emergency wireless networking in the aftermath of disasters [6], among others. The foreseen wide adoption of UAV systems can pose a significant burden on the capacity of the underlying wireless networks.In this paper, we aim to explore new approaches that can enable UAV operations in the 6 GHz band to harvest the additional 1.2 GHz spectrum bandwidth [7].

The primary challenge towards this goal is in the spectrum sharing approaches adopted by the incumbent systems in this frequency band. The 6 GHz band consists of four sub-bands, i.e., U-NII-5 (5.925-6.425 GHz), U-NII-6 (6.425-6.525 GHz), U-NII-7 (6.525-6.875 GHz), and U-NII-8 (6.875-7.125 GHz). These bands have been previously occupied by a set of non-government services, including fixed point-to-point services, fixed-satellite service (Earth-to-space), broadcast auxiliary services and cable television relay services [7]. These incumbent systems coexist with each other by sharing the spectrum on a directional basis, i.e., they use highly directional antennas to concentrate the signal energy in a particular direction such that the mutual interference can be effectively mitigated as long as their antennas are not pointed toward each other. As a result, traditional carrier-sensing-based spectrum sharing as in Wi-Fi networks is not applicable to extend those wireless systems with omnidirectional antennas to this frequency band, because of the low detectability of the incumbent systems. For this reason, two operation modes have been proposed by the FCC, i.e., standard-power and low-power modes. The former allows both indoor and outdoor operations on the U-NII-5 and U-NII-7 bands with maximum transmission power of 30 dBm. The latter focuses on indoor operations in the U-NII-6 and U-NII-8 bands with maximum transmission power of 24 dBm.

However, neither of the above two modes supports UAV operations in the 6 GHz bands [7], [8]. A major concern is that the high mobility of the UAV systems makes it difficult to model and control their aggregate interference to the incumbent systems. The situation gets even worse when

considering the altitude-dependent interference range of UAVs and the higher probability of line-of-sight signal propagation at higher altitudes. Additionally, it is also challenging for the distributed UAVs to control their aggregate interference collaboratively by jointly considering their spectrum access strategies and association to the ground users.

To address these challenges, a key step is to understand the statistical behaviors and effects of the aggregate interference experienced by the incumbent systems, since no real-time cross-system channel state information (CSI) is available. To this end, in this paper we focus on a new spectrum sharing scenario in the 6 GHz band called *SwarmShare*, where a set of UAVs collaboratively provide data streaming services to ground users, by sharing the spectrum with the incumbent systems on the 6 GHz band under the cross-system interference constraints. Within this framework, we model and analyze the aggregate interference from the UAVs to the incumbent users, and propose a mobility-resilient stochastic spectrum sharing approach, based on which the interference can be mitigated from the coexisting UAV networks to the incumbent users in the 6 GHz band, while increasing the SINR of the UAV networks. The main contributions of this work are as follows:

- We first present a mathematical formulation of the *SwarmShare* problem, where the objective is to maximize the spectral efficiency of the wireless UAV network by jointly controlling the UAVs' transmission power and flight trajectory as well as their association to the ground users, under the interference constraints of the incumbent system. It is shown that the resulting problem is a mixed integer nonlinear non-convex programming (MINLP) problem.
- We analyze the statistical behavior of the aggregate interference from the UAVs to the incumbent system, and find that no existing models can be used to characterize the statistical behavior of the interference. With this observation, we propose to solve the above MINLP spectrum sharing problem following a data-driven three-phase approach: *Initial Power Enforcement*, *Offline-dataset Guided Online Power Adaptation*, and *Reinforcement Learning-based UAV Optimization*.
- We validate the effectiveness of *SwarmShare* by conducting an extensive simulation campaign over UBSim, a newly developed Universal Broadband Simulator for integrated aerial-ground wireless networks. It is found that, with *SwarmShare*, effective spectrum sharing can be achieved *without* real-time cross-system channel state information and, which is somewhat surprising, even with *no* precise location information of the UAVs.

The rest of the paper is organized as follows. In Sec. II, we discuss the related works. The system model and problem formulation are presented in Sec. III. In Sec. IV, we describe the spectrum sharing framework. Performance evaluation results are discussed in Sec. V and finally we draw the main conclusions in Sec. VII.

II. Related Work

UAV systems have attracted significant research attention in both academia and industry [2], [9], [10], [11], [12], [13]. For example, in [2] the authors optimize the achievable rate of UAV-aided cognitive IoT networks. Wang et al. propose in [9] a dynamic hyper-graph coloring approach for spectrum sharing in UAV-assisted networks. In [10], the authors optimize mobile terminals' throughput by jointly controlling UAV trajectory, bandwidth allocation and user partitioning between the UAV and ground base stations. In [11], a UAV is used as a relay to assist D2D communications. In [12], the authors studies machine learning based spectrum sharing for UAV-assisted emergency communications. The authors of [13] adopt UAVs to harvest the primary RF signal as an energy source of the secondary users. Readers are referred to [14] and [15] and references therein for a survey of the main results in this area.

Spectrum sharing in cognitive radio networks has also been a hot research topic for a long time with a sizable and increasing body of literature. In [16], the authors aim to maximize the average secrecy rate of the secondary network by robustly optimizing the UAV's trajectory and transmit power. In [17], the authors maximize the revenue of the newly joined systems in cognitive radio networks by controlling the channel access of new users. The authors of [18] propose a cognitive backscatter network to maximize the data rate of the newly joined networks. By leveraging recent advances in MIMO, the authors enable transparent spectrum sharing for a small cognitive radio network in [19]. A deep reinforcement learning based power control scheme is designed in [20] to meet the QoS requirements of both primary and secondary users. Based on a combination of model-free and model-based reinforcement learning, the authors of [21] propose a dynamic spectrum access scheme for secondary users with imperfect sensing.

Spectrum sharing between directional- and omnidirectional-antenna wireless systems has also been studied in existing literature. For example, authors in [22] optimize the performance of LTE-Unlicensed networks while guaranteeing the performance of the co-located radar system. The authors of [23] propose RadChat, a distributed networking protocol for mitigation of interference among frequency modulated continuous wave radars. A cooperative spectrum sharing model is proposed in [24] to mitigate the mutual interference among radar and communication systems. In [25], the authors propose a framework for spectrum sharing between satellite and terrestrial networks and analyze the interference in both downlink and uplink from terrestrial cellular systems and nongeostationary systems to geostationary systems within the framework. Please refer to [26] and [27] and references therein for a good survey of the main results in this field.

Further comparison of the above discussed references in different aspects is summarized in Table I. From the table, it can be seen that no existing work considers spectrum sharing in the 6 GHz band between directional and omnidirectional mobile wireless communication systems. Differently, we instead aim to *design a new, mobility-resilient spectrum sharing framework between UAVs and the incumbent wireless systems in the 6 GHz band to improve spectral efficiency and maximize the throughput of the UAV network for*

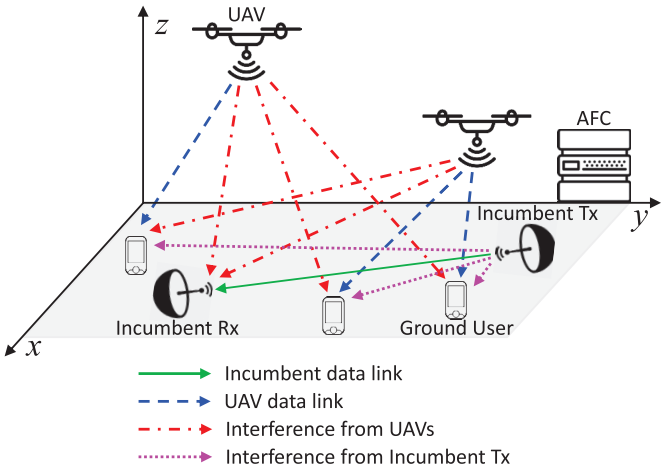

Fig. 1. Spectrum sharing between coexisting UAV network and the incumbent network in the 6 GHz bands.

elastic applications such as data collection, file transfer and messages.

III. System Model and Problem Formulation

As shown in Fig. 1, we consider a wireless UAV network coexisting with an incumbent communication pair (Tx and Rx) by sharing the same portion of spectrum B in the 6 GHz band. The UAV network consists of a set $\mathcal{K}$ of UAVs collaborating with each other to serve a set $\mathcal{M}$ of ground users. The transmission time is divided into a set $\mathcal{T}$ of consecutive time slots. In each time slot $t \in \mathcal{T}$, denotes the coordinate vector of UAV $k \in \mathcal{K}$ as $\mathbf{cod}_k^t = [x_k^t, y_k^t, z_k^t]^{\mathrm{T}}$, with T being the transpose operation and x_k^t, y_k^t and z_k^t representing the x-, y- and z-axis components, respectively. Similarly, denote respectively $\mathbf{cod}_{\mathrm{Tx}} = [x_{\mathrm{Tx}}, y_{\mathrm{Tx}}, z_{\mathrm{Tx}}]^{\mathrm{T}}$, $\mathbf{cod}_{\mathrm{Rx}} = [x_{\mathrm{Rx}}, y_{\mathrm{Rx}}, z_{\mathrm{Rx}}]^{\mathrm{T}}$ and $\mathbf{cod}_i = [x_i, y_i, z_i]^{\mathrm{T}}$ as the coordinate vectors of incumbent transmitter Tx, incumbent receiver Rx and ground node $i \in \mathcal{M} \cup \{\mathrm{Tx}, \mathrm{Rx}\}$. Denote $\mathcal{A} = \mathcal{K} \cup \mathcal{M} \cup \{\mathrm{Tx}, \mathrm{Rx}\}$ as the set of all the nodes in the heterogeneous network. The objective of the UAV network is to maximize its own spectral efficiency under the interference constraints of the incumbent system. Before presenting the formal formulation of the spectrum sharing problem, we first describe the considered channel, antenna and throughput models.

A. Channel Model

We consider both large-scale path-loss and small-scale fading. For path-loss, we consider line-of-sight (LoS) wireless channels between the incumbent transmitter Tx and its receiver Rx. This is feasible because the incumbent systems are usually carefully deployed such that their antennas are well-aligned without any obstructions in the link. We consider non-line-of-sight (NLoS) links between the incumbent nodes and the ground users of the coexisting networks. For UAV networks, we consider both LoS and NLoS links. Specifically, we consider as in [28] a probabilistic path-loss model for the links between UAVs and ground nodes. Then, the LoS and NLoS path-loss (in dB) between UAV $k \in \mathcal{K}$ and ground node $i \in \mathcal{M} \cup \{\mathrm{Tx}, \mathrm{Rx}\}$ can be given as, in time slot $t \in \mathcal{T}$,

$$H_{ki}^{\mathrm{LoS},t} = 20 \log \left(\frac{4\pi d_{ki}^t f}{c} \right) + \eta^{\mathrm{LoS}}, \tag{1}$$

$$H_{ki}^{\mathrm{NLoS},t} = 20 \log \left(\frac{4\pi d_{ki}^t f}{c} \right) + \eta^{\mathrm{NLoS}}, \tag{2}$$

where the first term on the right-hand side of (1) and (2) represents the free space path-loss with $d_{ki}^t = ||\mathbf{cod}_k^t - \mathbf{cod}_i||_2$ being the distance between UAV k and receiver i in time slot t, f is the carrier frequency of UAV k, c is the speed of light, and η^{LoS} and η^{NLoS} are the additional attenuation factors due to LoS and NLoS transmissions, respectively. Let $\Pr(H_{ki}^{\mathrm{LoS},t})$ represent the probability of LoS transmissions in time slot t, then $\Pr(H_{ki}^{\mathrm{LoS},t})$ can be expressed as [29],

$$\Pr(H_{ki}^{\mathrm{LoS},t}) = (1 + X \exp(-Y[\phi_{ki} - X]))^{-1}, \tag{3}$$

where X and Y are given environment-dependent constants and $\phi_{ki} = \sin^{-1}(z_k^t / d_{ki}^t)$. Accordingly, the probability of NLoS transmissions between UAV $k \in \mathcal{K}$ and receiver $i \in \mathcal{M} \cup \{\mathrm{Tx}, \mathrm{Rx}\}$ can be given as $\Pr(H_{ki}^{\mathrm{NLoS},t}) = 1 - \Pr(H_{ki}^{\mathrm{LoS},t})$.

Finally, for small-scale fading we consider Rician fading for LoS transmissions and Rayleigh fading for NLoS. Denote K_{ij} as the Rician factor for the wireless channel between nodes $i, j \in \mathcal{A}$, then K_{ij} can be given as $K_{ij} = 13 - 0.03\, d_{ij}$ for LoS transmissions and 0 for NLoS, where d_{ij} is the distance between the two nodes. Denote the resulting small-scale fading coefficient as $h_{ij}^t \triangleq h_{ij}^t(K_{ij})$ for nodes $i, j \in \mathcal{A}$.

B. Antenna Model

As described in Sec. I, in this work we consider directional transmissions for the incumbent wireless systems and omnidirectional transmissions for the coexisting UAV network. Specifically, we consider as in [30] a bi-sectorized antenna model to characterize the interference between directional and omnidirectional antennas. Denote θ_{Tx} and θ_{Rx} as the signal beamwidth of the incumbent transmitter and receiver's antennas, respectively. Let $\theta_m \in [-\pi, \pi]$ denote the offset angle of the boresight direction of the Tx's antenna with respect to the reference direction for ground user $m \in \mathcal{M}$. Here, the reference direction refers to the direction along which the Tx's antenna would be exactly pointed to user m. Then the antenna gain of incumbent transmitter Tx with respect to ground user $m \in \mathcal{M}$ in time slot t, denoted as $w_{m\mathrm{Tx}}^t$, can be written as

$$w_{m\mathrm{Tx}}^t = \begin{cases} w_{\mathrm{Tx}}^{\max}, & \text{if } \theta_m \le \theta_{\mathrm{Tx}} \\ w_{\mathrm{Tx}}^{\min}, & \text{otherwise} \end{cases}, \tag{4}$$

where $w_{\mathrm{Tx}}^{\max}$ and $w_{\mathrm{Tx}}^{\min}$ represent the maximum and minimum transmit gains of the incumbent transmitter, respectively. Similarly, the receive gain of the incumbent receiver Rx with respect to UAV $k \in \mathcal{K}$, denoted as $w_{k\mathrm{Rx}}^t$, can be given as

$$w_{k\mathrm{Rx}}^t = \begin{cases} w_{\mathrm{Rx}}^{\max}, & \text{if } \theta_k \le \theta_{\mathrm{Rx}} \\ w_{\mathrm{Rx}}^{\min}, & \text{otherwise} \end{cases}, \tag{5}$$

with $w_{\mathrm{Rx}}^{\max}$ and $w_{\mathrm{Rx}}^{\min}$ being the maximum and minimum receive gains of the incumbent receiver, respectively. The

TABLE I
COMPARISON OF RELATED WORK IN DIFFERENT ASPECTS

Reference	Spectrum Band	Mobility Support	Antenna Type	Performance Metric
[2]	2.4 GHz	Yes	Omnidirectional	Throughput
[9]	Unknown	Yes	Omnidirectional	User Number
[10]	Unknown	Yes	Omnidirectional	Throughput
[11]	Unknown	Yes	Omnidirectional	Throughput
[12]	2 GHz	Yes	Omnidirectional	Throughput
[13]	840.5 - 845.5 MHz	No	Omnidirectional	Secrecy Outage Probability
[16]	Unknown	Yes	Omnidirectional	Throughput
[17]	Unknown	No	Omnidirectional	Throughput
[18]	Unknown	No	Omnidirectional	Throughput
[19]	2.48 GHz	No	Omnidirectional	Interference
[20]	Unknown	No	Omnidirectional	Throughput
[21]	Unknown	No	Omnidirectional	Sample Efficiency
[22]	5 GHz	No	Directional	Power
[23]	Unknown	No	Directional	Interference
[24]	Below 100 MHz	No	Directional	Throughput
[25]	18 GHz	No	Directional	Interference

transmit and receive gains are set to the maximum values for incumbent transmissions, i.e., $w_{\mathrm{Tx}}^{\max}$ and $w_{\mathrm{Rx}}^{\max}$, respectively.

C. Throughput Model

Based on the above channel and antenna models, the signal-to-interference-plus-noise ratio (SINR) of the incumbent receiver Rx, denoted as γ_{Rx}^t for time slot t, can be written as

$$\gamma_{\mathrm{Rx}}^t = \frac{p_{\mathrm{Tx}} w_{\mathrm{Tx}}^{\max} w_{\mathrm{Rx}}^{\max} \cdot (h_{\mathrm{TxRx}}^t)^2 / H_{\mathrm{TxRx}}^{\mathrm{LoS}}}{\sum\limits_{k\in\mathcal{K}} p_k^t w_{k\mathrm{Rx}}^t w_k \cdot (h_{k\mathrm{Rx}}^t)^2 / H_{k\mathrm{Rx}}^t + (\sigma_{\mathrm{Rx}})^2} \tag{6}$$

where p_{Tx} and p_k^t represent the transmission power of the incumbent transmitter Tx and UAV $k \in \mathcal{K}$ in time slot $t \in \mathcal{T}$, respectively; w_k denotes the transmit gain of the UAV and is considered to be constant for omnidirectional antennas; and $(\sigma_{\mathrm{Rx}})^2$ is the power of Additive White Gaussian Noise (AWGN) at the incumbent receiver.

The objective of *SwarmShare* is to guarantee satisfactory SINR for the incumbent system (i.e., γ_{Rx}^t) by controlling the transmission power of the coexisting UAVs. To this end, we consider a single-home association strategy for the ground users of the UAV network, i.e., in each time slot $t \in \mathcal{T}$ each ground user can be served by at most one UAV. Denote α_{km} as the association variable, with $\alpha_{km} = 1$ if ground user $m \in \mathcal{M}$ is associated with UAV $k \in \mathcal{K}$ and $\alpha_{km} = 0$ otherwise. Then we have

$$\sum_{k\in\mathcal{K}} \alpha_{km}^t \le 1, \forall k \in \mathcal{K}, m \in \mathcal{M}, t \in \mathcal{T} \tag{7}$$

$$\alpha_{km}^t \in \{0,1\}, \forall k \in \mathcal{K}, m \in \mathcal{M}, t \in \mathcal{T} \tag{8}$$

Denote $\mathcal{M}_k^t \triangleq \{m | m \in \mathcal{M}, \alpha_{km}^t = 1\}$ as the set of ground users served by UAV k in time slot t.

We further consider FDMA-based spectrum access among the UAVs in $\mathcal{K}$ and TDMA for the ground users served by the same UAV. Then, the SINR of ground user $m \in \mathcal{M}$ in time slot t, denoted as $\gamma_m^t = \gamma_m^t(H_{m\mathrm{Tx}}^t)$ can be expressed as

$$\gamma_m^t = \frac{p_{k(m)}^t \cdot (h_{k(m)m}^t)^2 / H_{k(m)m}^t}{(p_{\mathrm{Tx}}/|\mathcal{K}|) \cdot w_{m\mathrm{Tx}}^t \hat{w}_m \cdot (h_{m\mathrm{Tx}}^t)^2 / (H_{m\mathrm{Tx}}^t) + \sigma_m^2}, \tag{9}$$

where $k(m)$ and $\hat{w}_m$ represent the serving UAV and receive gain of ground user m, respectively; $|\mathcal{K}|$ denotes the number of UAVs in $\mathcal{K}$; $H_{k(m)m}^t \in \{H_{k(m)m}^{\mathrm{NLoS},t}, H_{k(m)m}^{\mathrm{LoS},t}\}$ is the path-loss from UAV $k(m)$ to ground user m in time slot t with $H_{k(m)m}^{\mathrm{NLoS},t}$ and $H_{k(m)m}^{\mathrm{LoS},t}$ defined in Sec. III-A; and σ_m^2 is the power of the AWGN noise at ground user m. Notice in (9) that only $\frac{1}{|\mathcal{K}|}$ of the incumbent transmitter's power (i.e., $p_{\mathrm{Tx}}/|\mathcal{K}|$) is considered for each UAV and its associated ground users because of the UAVs' FDMA-based spectrum access. It is worth pointing out that we consider FDMA- and TDMA-based spectrum access for the UAV networks because we want to focus this work on the interference control between the UAV and the incumbent systems. The resulting cross-system spectrum sharing scheme can also be extended to other more advanced spectrum access schemes for UAVs [31], [32].

Finally, the capacity achievable by user m in time slot t, denoted as $C_{k(m)m}^t$, can be expressed as

$$\begin{aligned} C_{k(m)m}^t &= \frac{B}{|\mathcal{K}||\mathcal{M}_k^t|}\Big[\Pr\left(H_{k(m)m}^{\mathrm{NLoS},t}\right)\log_2\left(1+\gamma_m^t(H_{k(m)m}^{\mathrm{NLoS}})\right) \\ &\quad + \Pr\left(H_{k(m)m}^{\mathrm{LoS},t}\right)\log_2\left(1+\gamma_m^t(H_{k(m)m}^{\mathrm{LoS}})\right)\Big], \end{aligned} \tag{10}$$

where $\Pr(\cdot)$ is the probability of LoS and NLoS transmissions defined in Sec. III-A and $\gamma_m^t(\cdot)$ is the SINR of ground user m defined in (9).

D. Problem Formulation

Define $\mathbf{P} = (p_k^t)_{k\in\mathcal{K}}^{t\in\mathcal{T}}$ as the transmission power vector of the UAVs, $\mathbf{A} = (\alpha_{km}^t)_{k\in\mathcal{K},m\in\mathcal{M}}^{t\in\mathcal{T}}$ as the UAV-user association vector, and $\mathbf{Q} = (\mathbf{cod}_k^t)_{k\in\mathcal{K}}^{t\in\mathcal{T}}$ as the UAV location vector. Then the objective of the *SwarmShare* control problem is

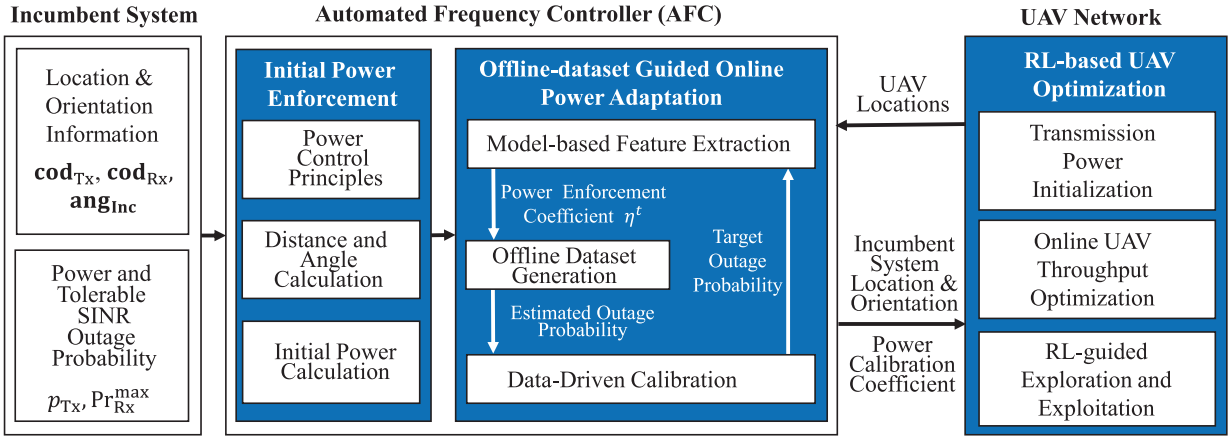

Fig. 2. Diagram of the *SwarmShare* spectrum sharing framework.

to maximize the aggregate capacity of the UAV network by jointly controlling the transmission power of the UAVs and their flight trajectory as well as association with the ground users, while meeting the cross-system interference constraints, as formulated as

$$\underset{\mathbf{P},\,\mathbf{A},\,\mathbf{Q}}{Maximize} \quad \frac{1}{|\mathcal{T}|}\sum_{t\in\mathcal{T}}\sum_{m\in\mathcal{M}} C^t_{k(m)m} \tag{11}$$

$$\text{Subject to}: \quad 0 \le p_k^t \le p_{\max}, \forall k \in \mathcal{K}, t \in \mathcal{T}, \tag{12}$$

$$Association\ Constraints\ (7),\ (8) \tag{13}$$

$$\underbrace{\frac{1}{|\mathcal{T}|}\sum_{t\in\mathcal{T}} \mathrm{I}(\gamma_{\mathrm{Rx}}^t \le \gamma_{\mathrm{Rx}}^{\mathrm{th}}) \le \mathrm{Pr}_{\mathrm{Rx}}^{\max}}_{Cross-system\ Interference\ Constraint} \tag{14}$$

where $C^t_{k(m)m}$ is defined in (10), $p_{\max}$ is the maximum transmission power of each UAV, $\mathrm{I}(\cdot)$ is the indication function taking value of 1 if the condition holds and 0 otherwise, and $\gamma_{\mathrm{Rx}}^{\mathrm{th}}$ and $\mathrm{Pr}_{\mathrm{Rx}}^{\max}$ denote respectively the threshold SINR and the maximum tolerable SINR outage probability of the incumbent system.

IV. Spectrum Coexistence Design

The *SwarmShare* problem formulated in (11)-(14) is a mixed integer nonlinear nonconvex programming (MINLP) problem, because of the binary UAV-user association variables α_{km}^t and the underlying complicated mathematical expressions in (11) and (14). Moreover, to solve the problem directly it requires knowing the real-time channel state information (CSI) between the UAV network and the incumbent system, which is unavailable, as discussed in Sec. I, because of the low-detectability of the directional incumbent signals.

To address the above challenges, in this work we consider an AFC (Automated Frequency Controller)-assisted spectrum sharing. AFC has been adopted for spectrum sharing in the TV whitespace band as well as the 6 GHz band by determining certain exclusion zones nearby the incumbent systems [7]. Our work differs from this with our objective to enable exclusion-zone-free hence more flexible spectrum sharing, and study the statistical behavior of the aggregate interference from the UAV networks to the incumbent system, while keeping the cross-system signaling at a minimum level. The diagram of the proposed spectrum coexistence framework is illustrated in Fig. 2, where there are three major components, i.e., *Initial Power Enforcement*, *Offline-dataset Guided Online Power Adaptation*, and *Reinforcement Learning-based UAV Optimization*.

A. Initial Power Enforcement

The objective of this phase is to determine, following a set of *Power Control Principles*, a rough transmission power for each of the UAVs. In this work, we consider three basic principles to accommodate the effects of the UAVs' flight altitudes and their locations on the interference to the incumbent system, while more sophisticated principles can be incorporated in the future. These principles are i) UAVs that are closer to the incumbent receiver should transmit at lower power; (ii) with the same distance to the incumbent receiver, UAVs flying higher should transmit at lower power; and (iii) with the same distance and altitude, UAVs with smaller angles relative to the boresight axis of the incumbent receivers' directional antenna should transmit at lower power. Particularly, the rationale of the second principle is that, with the hybrid LoS/NLoS channel model described in Sec. III-A, it is more likely for a UAV to establish LoS links to the incumbent receiver when flying higher and hence cause more interference. Similarly, for the third principle, based on the directional antenna model described in Sec. III-B, a UAV will cause higher interference when it is more aligned with the incumbent receiver's antenna.

In *SwarmShare*, an initial power enforcement coefficient, denoted as $\mathrm{Enf}(\mathbf{cod}_k^t, \mathbf{cod}_{\mathrm{Rx}}, \mathbf{ang}_{\mathrm{Inc}})$, will be calculated for each UAV $k \in \mathcal{K}$ in time slot $t \in \mathcal{T}$ based on the above three principles. This is accomplished using three Sigmoid-family functions $Sig_1(\cdot)$, $Sig_2(\cdot)$ and $Sig_3(\cdot)$, as follows:

$$\mathrm{Enf}(\mathbf{cod}_k^t, \mathbf{cod}_{\mathrm{Rx}}, \mathbf{ang}_{\mathrm{Inc}}) = \underbrace{Sig_1\left(\frac{l_{\mathrm{euc}}(\mathbf{cod}_k^t, \mathbf{cod}_{\mathrm{Rx}})}{l_{\mathrm{euc}}^{\mathrm{th}}}\right)}_{Principle\ 1}$$

$$\cdot \underbrace{Sig_2\left(\frac{h(\mathbf{cod}_k^t)+h(\mathbf{cod}_{\mathrm{Rx}})}{l_{\mathrm{hgh}}^{\mathrm{th}}}\right)}_{Principle\ 2} \cdot \underbrace{Sig_3\left(l_{\mathrm{rad}}(\mathbf{cod}_k^t,\mathbf{cod}_{\mathrm{Rx}},\mathbf{ang}_{\mathrm{Inc}})\right)}_{Principle\ 3}, \quad (15)$$

where $l_{\mathrm{euc}}(\cdot,\cdot)$ represents the Euclidean distance between UAV k and the incumbent receiver given their coordinates; $h(\cdot)$ represents their height, and $l_{\mathrm{rad}}(\cdot,\cdot,\cdot) \in [0,\pi]$ is the angle (in radians) of UAV k with respect to the boresight axis of the incumbent receiver antenna; finally, $l_{\mathrm{euc}}^{\mathrm{th}}$ and l_{hgh}^{th} in equation (15) are respectively, the threshold distance and height beyond which $Sig_1(\cdot)$ and $Sig_2(\cdot)$ become nearly constant. It is worth pointing out that, since a standard sigmoid function is a differentiable, monotonically increasing, real function taking values in $[0,1]$, we design $Sig_1(\cdot)$, $Sig_2(\cdot)$ and $Sig_3(\cdot)$ by scaling, shifting and reversing the standard sigmoid function to consider the effects of the UAV location, flight altitude and relative angle to the incumbent receiver. For example, $Sig_1(x) = \frac{1}{1+e^{-3(x/70-2)}}$ has been adopted for principle 1 in this work, while $Sig_2(\cdot)$ and $Sig_3(\cdot)$ can be defined similarly. With the obtained power enforcement coefficient $\mathrm{Enf}(\mathbf{cod}_k^t,\mathbf{cod}_{\mathrm{Rx}},\mathbf{ang}_{\mathrm{Inc}})$, each UAV's power can be initialized as, in time slot $t \in \mathcal{T}$,

$$p_k^{\mathrm{ini}} = p^{\max}\mathrm{Enf}(\mathbf{cod}_k^t,\mathbf{cod}_{\mathrm{Rx}},\mathbf{ang}_{\mathrm{Inc}}),\ \forall k \in \mathcal{K}, \quad (16)$$

where $p^{\max}$ is the maximum transmission power of each UAV.

B. Offline-Dataset Guided Online Power Adaptation

Recall in Sec. III that our goal is to enable UAV operations in the 6 GHz band while meeting the cross-system interference constraint (14). In *SwarmShare*, this is accomplished by fine-tuning the above obtained initial transmission power for the UAVs according to a three-step approach, as described as follows.

1) Model-Based Feature Extraction: In this step, we first extract the network features that can be used later in *Data-Driven Calibration*, rather than using directly, the raw network topology information such as UAV location vector $(\mathbf{cod}_k^t)_{k\in\mathcal{K}}^{t\in\mathcal{T}}$. It is important to mitigate the curse of dimensionality problem [33] especially with a large number of UAVs. In *SwarmShare*, we select the power adaptation coefficient, denoted as η^t for time slot t, as the network feature. Then, given the above obtained initial transmission power p_k^{ini} for UAV $k \in \mathcal{K}$, a new transmission power p_k^t can be obtained as

$$p_k^t = \begin{cases} 0, & \text{if } \alpha_{km}^t = 0, \forall m \in \mathcal{M} \\ p_k^{\mathrm{ini}}\eta^t, & \text{otherwise} \end{cases}. \quad (17)$$

That is, the transmission power will be set to 0 if a UAV is not associated to any ground users. Then the interference constraint (14) can be rewritten as

$$\frac{1}{|\mathcal{T}|}\sum_{t\in\mathcal{T}} \mathrm{I}(\gamma_{\mathrm{Rx}}^t(\eta^t) \le \gamma_{\mathrm{Rx}}^{\mathrm{th}}) \le \mathrm{Pr}_{\mathrm{Rx}}^{\max}, \quad (18)$$

where $\gamma_{\mathrm{Rx}}^t(\eta^t)$ is the SINR of the incumbent receiver defined in (6) by substituting (17) into (6). Consider an ergodic stochastic process for the aggregate interference and denote $\mathrm{Prob}(\gamma_{\mathrm{Rx}}^t(\eta^t) \le \gamma_{\mathrm{Rx}}^{\mathrm{th}})$ as the SINR outage probability in time slot $t \in \mathcal{T}$, then the left-hand side of (18) can be equivalently represented as

$$\mathrm{Prob}(\gamma_{\mathrm{Rx}}^t(\eta^t) \le \gamma_{\mathrm{Rx}}^{\mathrm{th}}) \quad (19)$$

$$= \mathrm{Prob}\left(\frac{P_{\mathrm{Rx}}^{\mathrm{sig}}}{P_{\mathrm{Rx}}^{\mathrm{itf}}} \le \gamma_{\mathrm{Rx}}^{\mathrm{th}}\right) \quad (20)$$

$$= \int_0^{+\infty}\int_{\frac{P_{\mathrm{Rx}}^{\mathrm{sig}}}{\gamma_{\mathrm{Rx}}^{\mathrm{th}}}}^{+\infty} \underbrace{\mathrm{pdf}_{P_{\mathrm{Rx}}^{\mathrm{sig}}}(p^{\mathrm{sig}})}_{\substack{Noncentral\\ Chi-square\\ Distribution}} \cdot \underbrace{\mathrm{pdf}_{P_{\mathrm{Rx}}^{\mathrm{itf}}}(p^{\mathrm{itf}})}_{\substack{Gamma\\ Distribution}} \mathrm{d}p^{\mathrm{itf}}\mathrm{d}p^{\mathrm{sig}}, \quad (21)$$

where $P_{\mathrm{Rx}}^{\mathrm{sig}}$ and $P_{\mathrm{Rx}}^{\mathrm{itf}}$ are the numerator and denominator of (6), respectively; a Rayleigh distribution has been considered for the small-scale fading and hence noncentral chi-square distribution [34] for the receive power of the incumbent signals; and finally as in [35] and [36] a Gamma distribution is considered for the aggregate interference power. It is worth pointing out that, as shown later in Sec. V, the aggregate interference of UAVs does not follow any existing statistical distributions. In this work, we consider the Gamma distribution in (21) because we want to obtain a rough estimation of the power adaptation coefficient η^t, which will be further calibrated based on an offline dataset. Notice that given the maximum tolerable SINR outage probability $\mathrm{Pr}_{\mathrm{Rx}}^{\max}$ in (18), the maximum η^t can be determined efficiently by bisection search, since the left-hand side of (18), which is equivalent to (21), is a monotonically increasing function of the UAVs' transmission power hence η^t.

2) Offline-Dataset Generation: Given the above obtained network feature η^t, each UAV's transmission power p_k^t can be updated according to (17). Since the power adaptation may be inaccurate because of the inaccuracy of the Gamma distribution-based interference model in (21), we further calibrate the power control for UAVs with the assistance of offline measurements. Specifically, given the transmission power vector $(p_k^t)_{k\in\mathcal{K}}$, the corresponding SINR outage probability of the incumbent system can be obtained by offline simulations. By varying the number of UAVs, their locations, as well as the maximum tolerable SINR outage probability in the simulations, we are able to obtain an SINR outage probability vector. Denote $\mathbf{Pr}_{\mathrm{Rx}}^{\max} = (\mathrm{Pr}_{\mathrm{Rx}}^{\max})$ as the vector of the maximum tolerable outage probability, and accordingly denote the simulated outage probability vector as $\overline{\mathbf{Pr}}_{\mathrm{Rx}}^{\max}(\boldsymbol{\eta}) = (\overline{\mathrm{Pr}}_{\mathrm{Rx}}^{\max}(\eta^t))$ with $\overline{\mathrm{Pr}}_{\mathrm{Rx}}^{\max}(\eta^t)$ being the SINR outage probability given the network metric η^t, and $\boldsymbol{\eta} = (\eta^t)$ the network feature vector.

3) Data-Driven Calibration: Finally, a mapping between $\mathbf{Pr}_{\mathrm{Rx}}^{\max}$ and $\overline{\mathbf{Pr}}_{\mathrm{Rx}}^{\max}(\boldsymbol{\eta})$ can be established through function approximation, e.g., based on linear regression [37], echo state learning [38] or deep neural networks [20]. In this work we find that it is enough to approximate the mapping based on linear regression. Denote the mapping as $\mathrm{Pr}_{\mathrm{Rx}}^{\max} = f(\overline{\mathrm{Pr}}_{\mathrm{Rx}}^{\max}(\eta^t))$. Then, given $\overline{\mathrm{Pr}}_{\mathrm{Rx}}^{\max}$, the value of $\mathrm{Pr}_{\mathrm{Rx}}^{\max}$ and the corresponding network feature η^t can be obtained at network run time and further used for UAV power control based on (17).

C. Reinforcement Learning-Based UAV Optimization

As illustrated in Fig. 2, the above obtained η^t will be broadcast to the UAVs, which will then calculate their transmission power based on (17). Meanwhile, the UAVs will update their flight and association strategies to serve their users with higher spectral efficiency. To this end, we consider as in [30] the shortest-distance-based association strategy. Then, in each time slot $t \in \mathcal{T}$ the association variables $\alpha_{k,m}$ defined in Sec. III can be determined as

$$\alpha_{k,m} = \begin{cases} 1, & \text{if } k = \arg\min_{k} \|\mathbf{cod}_k^t - \mathbf{cod}_m\|^2 \\ 0, & \text{otherwise} \end{cases}. \quad (22)$$

Finally, as in [39], reinforcement learning with the ϵ-greedy search is adopted to guide the exploitation and exploration during the UAV's flight control. To this end, we further divide the whole network area into a set of three dimensional rectangles, each corresponding to a state of the RL control problem. Denote $\mathcal{S}$ as the set of all possible states. In each time slot, each UAV is allowed to either move to one of its adjacent rectangles or stay in the current. For each of the candidate rectangles, the UAV will first calculate the achievable capacity given the transmission power calculated in Sec. IV-A and IV-B and the set of ground users it serves.

Let $a \in \mathcal{A}$ be the action of the considered UAV, where $\mathcal{A} = \{F, B, U, D, R, L, S\}$ is the set of candidate actions, including moving forward, backward, upper, lower, right and left and staying at the current location. Then the action A_k^t chosen by UAV k at time slot t can be given by, for state $s \in \mathcal{S}$,

$$A_k^t = \begin{cases} \arg\max_{a \in \mathcal{A}} Q_k^t(a, s), & \text{with probability } 1 - \epsilon \\ a' \in \mathcal{A}/a, & \text{with probability } \dfrac{\epsilon}{|\mathcal{A}/a|} \end{cases}, \quad (23)$$

where $Q_k^t(a, s)$ is the estimated throughput value of UAV k if action a is chosen at state s in time t, and $|\cdot|$ represents the cardinality of a set. For each state, the state-action value (i.e., $Q_k^t(a, s)$) is estimated using a table-based approach with discount factor 0 [40]. Based on the selected action A_k^t at time slot t, coordinate vector $\mathbf{cod}_k^{t+1} = (x_k^{t+1}, y_k^{t+1}, z_k^{t+1})$ of UAV k for time slot $t+1$ can then be updated accordingly. The overall spectrum sharing algorithm is summarized in Algorithm 1.

Algorithm 1 SwarmShare Algorithm

Data: Node coordinates $\mathbf{cod}_i = (x_i, y_i, z_i); \forall i \in \mathcal{A}$, incumbent Tx transmission power p_{Tx}, tolerable SINR outage probability $\mathrm{Pr}_{\mathrm{Rx}}^{\max}$, total duration of simulation $\mathcal{T}$

Result: For each UAV $k \in \mathcal{K}$, the transmission power p_k^t for time slot $t \in \mathcal{T}$ and the coordinates $\mathbf{cod}_k^{t+1}$ for time slot $t+1 \in \mathcal{T}$

```
while t ∈ T do
    Initial Power Enforcement
    for each UAV k ∈ K do
        Calculate initial power enforcement coefficient Enf(·) based on (15); Calculate initial power p_k^ini based on (16);
    end
    Offline-dataset Guided Online Power Adaptation
    Determine the network feature η^t based on (18)-(21);
    for each UAV k ∈ K do
        Determine the transmission power p_k^t based on (17);
    end
    Reinforcement Learning-based UAV Optimization
    for each UAV k ∈ K do
        Determine the association variables α_{k,m} based on (22);
        Determine A_k^t based on (23) and update cod_k^{t+1} for next time slot.
    end
end
```

D. Complexity Analysis

The most time-consuming operation of Algorithm 1 is offline-dataset guided online power adaptation in Sec. IV-B. In Sec. IV-B.1, we need to determine the network feature η^t given the UAV network's topology and the maximum tolerable SINR outage probability. Since the SINR outage probability is a monotonically increasing function of η^t, the value of η^t can be obtained efficiently based on bisection search with a constant computational complexity for fixed range of η^t (i.e., [0, 1]) and the margin of error (1% in this work). It is worth pointing out that, for each iteration of bisection search, the AFC needs to calculate the mean and variance of the aggregate interference of UAVs given their current locations and their assigned transmission power based on (17). However, the resulting computational complexity is only negligible since it can be done by simple linear operations.

Finally, the dataset generation and regression in Sec. IV-B.2 can be conducted offline, and in Sec. IV-B.3 $\mathrm{Pr}_{\mathrm{Rx}}^{\max}$ can be determined online by solving a linear problem.

Regarding communication overhead, as illustrated in Fig. 2, in Sec. IV-A the AFC needs to collect one-time location and orientation information of the incumbent system and broadcast the collected information to the UAVs. If the incumbent system does not move frequently (which is usually the case, e.g., fixed point-to-point applications), the resulting communication overhead can be neglected. The AFC also needs to collect periodically the UAVs' locations and broadcast the updated power adaptation coefficient η^t to the UAVs. Since it is enough to represent this information in 16 bytes (three float numbers for location and one for the power adaptation coefficient, and each float number takes 4 bytes), the resulting broadcast overhead is low as well. Moreover, we will show later in Sec. V that the UAVs do not need to report their locations to the AFC in real-time, without obviously increasing the SINR

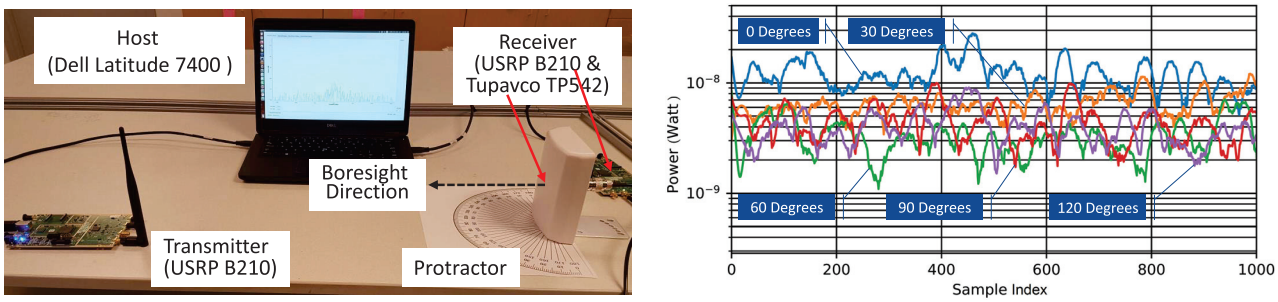

(a) (b)

Fig. 3. (a) Snapshot of the testbed setup for threshold angle measurement; (b) Examples of the measurement results.

outage probability of the incumbent system. This will further reduce the communication overhead.

V. Performance Evaluation

In this section we validate the effectiveness of the *SwarmShare* framework described in Sec. III and IV. We consider a network area of $500 \times 500 \times 50$ m^3, with 50 ground users randomly located in the network and the number of UAVs varying from 3 to 24. The incumbent transmitter and receiver are deployed with coordinates of (200, 200, 10) and (250, 250, 10), respectively. The center frequency of the shared spectrum is set to 6 GHz with a total bandwidth of 10 MHz. The maximum transmission power of the incumbent transmitter and the UAVs are set to 1 W and 0.25 W, respectively. For the bisectorized antenna model desribed in Sec. III, the maximum and minimum gains are set to 1 and 0.5, respectively. The power density of the AWGN is set to -174 dBm/Hz. The probability of LoS and NLoS links are set to 0.7 and 0.3, respectively. The threshold parameters $l_{\text{euc}}^{\text{th}}$ and $l_{\text{hgh}}^{\text{th}}$ in (15) are set to 70 m and 30 m, respectively. Next, before discussing the interference control results, we first determine the threshold angle for the directional antenna model described in Sec. III-B and validate the effectiveness of the data-driven calibration scheme proposed in Sec. IV-B.

A. Threshold Angle Measurement

We first determine the threshold angle for the directional antenna model described in Sec. III-B by conducting a set of experimental measurements. A snapshot of the testbed is shown in Fig. 3(a), where the transmitter is a USRP B210 software radio with an omnidirectional antenna, the receiver is another USRP B210 with a Tupavco TP542 antenna, and the baseband signal processing is conducted based on GNU Radio on a Dell Latitude 7400 laptop. Tupavco TP542 is a directional Wi-Fi antenna operating in a frequency range up to 5.8 GHz (very close to the 6 GHz band) with an antenna gain of 13 dBi. We measure the received power by varying the relative angle of the transmitter with respect to the boresight direction of the directional antenna (as illustrated in Fig. 3(a)) and the transmission distance from 1 to 3 meters. Examples of the measurement results are given in Fig. 3(b) with a transmission range of 1 meter and relative angles varying from 0 to 120 degrees at step of 30 degrees. The mapping between the received power and relative angle is established based on the logarithmic regression method [41]. Based on the regression results, we set 30 degree as the threshold angle for the bisectorized antenna model Sec. III-B, which corresponds to the 3 dB angle of the Tupavco TP542 antenna.

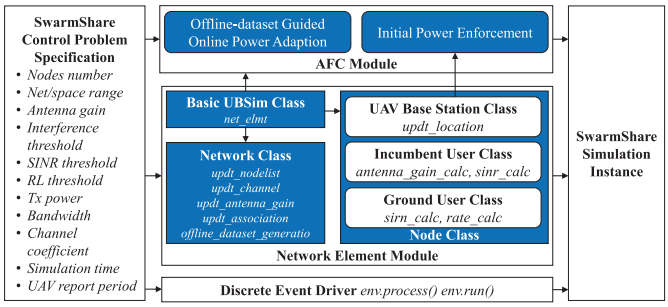

Fig. 4. Diagram of UBSim-based SwarmShare simulator.

B. Data-Driven Interference Prediction

Given the above obtained threshold angle, we further characterize the statistical behavior of the aggregate interference from the coexisting UAVs to the incumbent receiver. To this end, we conduct a set of simulations over UBSim, a newly developed Python-based Universal Broadband Simulator for integrated aerial-ground networking.[1] As shown in Fig. 4, the simulator consists of four major modules: *SwarmShare Control Problem Specification Module, AFC Module, Network Element Module* and *Discrete Event Driver.* The SwarmShare Control Problem Specification Module provides a set of APIs, based on which experimenters can define various network parameters such as the size of network area, the number of incumbent users, UAVs and ground users, antenna gain, probability channel coefficient, interference threshold, spectrum bandwidth, among others. Then, an object will be created for each of the incumbent users, UAV base stations and ground users in the *Network Element Module*. The classes of these network elements are defined in a hierarchical manner based on the basic network element class *net_elmt*, which defines

[1]In this work, the performance evaluation is conducted primarily over UBSim. We measure the threshold angle based on testbed experiments because in future work we want to further test the proposed spectrum coexistence framework in real world considering the directional antenna, Tupavco TP542, for incumbent users.

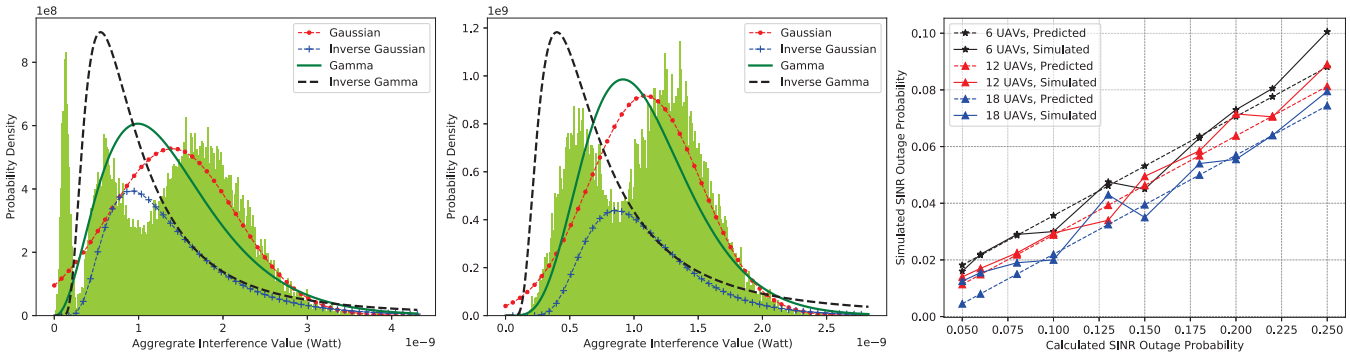

(a) (b) (c)

Fig. 5. Aggregate interference pdf with (a) 10 and (b) 20 UAVs; (c) Validation of data-driven prediction of the SINR outage probability for the incumbent system.

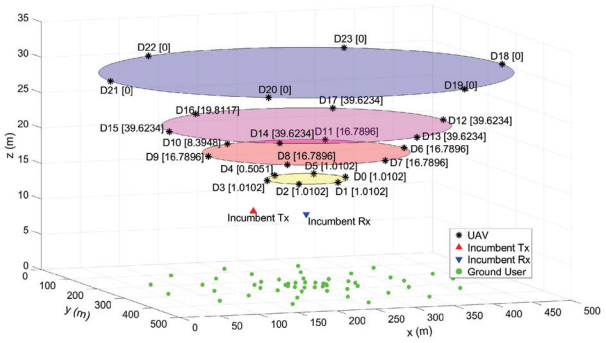

Fig. 6. Case study of power control based on *SwarmShare*. D#1[#2]: #1 is the UAV index, and #2 denotes the transmission power of the UAV in mW.

the most basic network element attributes and operations. The *AFC Module* is the place where the spectrum coordination algorithms designed in Sec. IV are deployed and executed. Finally, the *Discrete Event Driver* is developed based on the open-source library SimPy [42] for discrete event-driven simulations.

The results are reported in Figs. 5(a) and (b) with 10 and 20 UAVs, respectively. We fit as in [43] and [44] the collected interference values using four distributions, including Gaussian, Inverse Gaussian, Gamma and Inverse Gamma, and find that the power of the aggregate interference does not follow any of these distributions. This is actually our motivation to design *SwarmShare* based on a data-driven approach. Figure 5(c) reports the results of the data-driven prediction of the SINR outage probability. The offline dataset is generated based on simulations. We consider 6, 12 and 18 UAVs with multiple possible violation probabilities ranging from 0.05 to 0.25 with interval of 0.025. For each combination of UAV number and violation probability, we conduct 2000 episodes simulations with 2000 time slots in each episode. We can find that the predicted SINR outage probability matches the simulated results well.

C. Case Study

Fig. 6 shows an example of the power control results based on *SwarmShare*. To visualize the effects of the power control principles described in Sec. IV-A, in this example all the 24 UAVs are deployed uniformally along 4 circles with different altitudes and radii. From the figure, it can be seen that lower transmission powers have been allocated to UAVs along the lower circles. Also, because of the shorter distances from the incumbent receiver, lower transmission power has been allocated to the UAVs of the first circle from the bottom, e.g., 1.0102 mW for UAV 1 (i.e., D1[1.0102] in Fig. 6) against 16.7896 mW for UAV 7 and 39.6234 mW for UAV 13 along the second and third circles, respectively. Moreover, along the same circle, UAVs more aligned with the incumbent receiver have been allocated lower transmission powers, e.g., 8.3948 mW for UAV 10 vs 39.6234 mW for UAV 9 along the second circle. Finally, we notice in this example that all the UAVs along the fourth (i.e., the highest) circle have been allocated zero transmission power because no users are associated with them based on the shortest-distance association strategy described in Sec. IV-C. This also conforms to the third power control principle, i.e., with the same distance and relative angle, higher altitudes result in lower transmission powers because of higher probability of LoS transmissions. It is worth pointing out that the power allocation results are determined by jointly considering the three basic principles described in Sec. IV-A. In the following experiments, we will further evaluate the effectiveness of *SwarmShare* on the cross-system interference control.

In Figs. 7 and 8, we plot the instantaneous capacity achievable by the incumbent system and the UAV networks with different numbers of UAVs. In Fig. 7(a), we consider 6 hovering UAVs, and the maximum tolerable SINR outage probability is set to 0.05 for the incumbent system. The achievable capacity is plotted for 1000 time slots. Results indicate that the interference constraint of the incumbent system can be very well fulfilled, with SINR outage probability of 0.032. Similar results can be obtained with 12 and 18 hovering UAVs in Figs. 7(b) and (c), with the SINR outage probability of 0.029 and 0.021, respectively.

Fig. 8 shows the corresponding results with moving UAVs. In this experiment, the network area is divided into a set of three-dimension rectangles each of $50 \times 50 \times 10$ m^3. The trajectory of the UAVs are controlled as described in Sec. IV-C, with exploitation probability of 0.98. The same as in Fig. 7, the incumbent system's interference constraints can be satisfied in

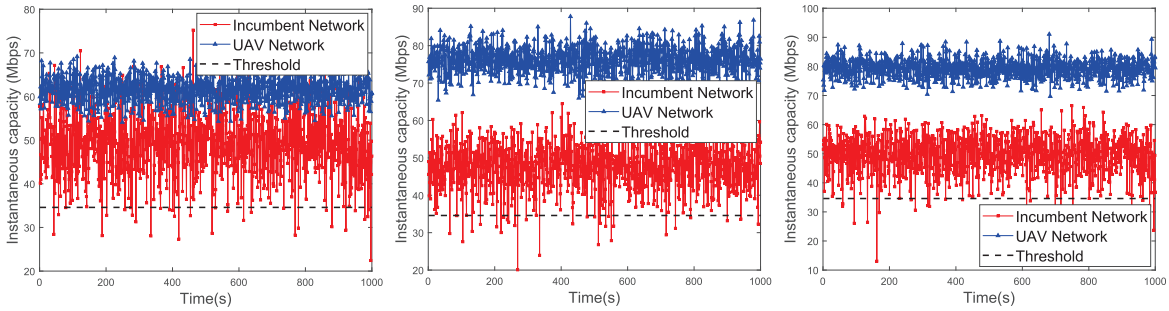

(a) 6 UAVs, Hovering (b) 12 UAVs, Hovering (c) 18 UAVs, Hovering

Fig. 7. Instantaneous capacity of the incumbent system and the UAV network with hovering UAVs. The violation probabilities are (a) 0.032, (b) 0.029 and (c) 0.021, respectively.

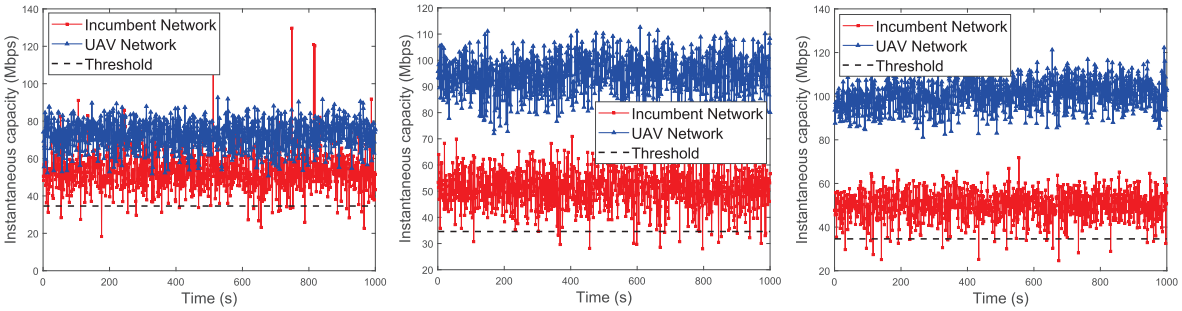

(a) 6 UAVs, Moving (b) 12 UAVs, Moving (c) 18 UAVs, Moving

Fig. 8. Instantaneous capacity of the incumbent system and the UAV network with moving UAVs. The violation probabilities are (a) 0.025, (b) 0.018 and (c) 0.022, respectively.

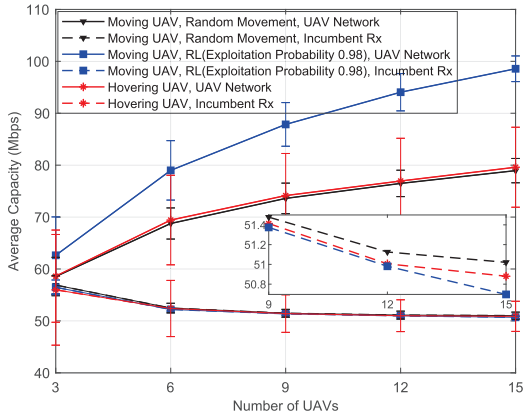

Fig. 9. Average capacity of the incumbent system and UAV networks with moving UAVs.

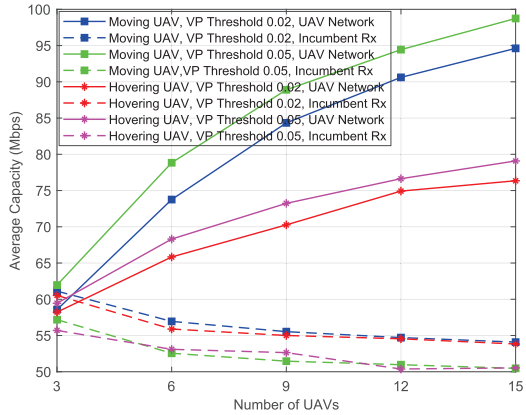

Fig. 10. Average capacity of the incumbent system and UAV networks with different violation probability (VP) threshold.

all the tested cases, with SINR outage probabilities of 0.025, 0.018 and 0.022 for 6, 12 and 18 UAVs, respectively, all below

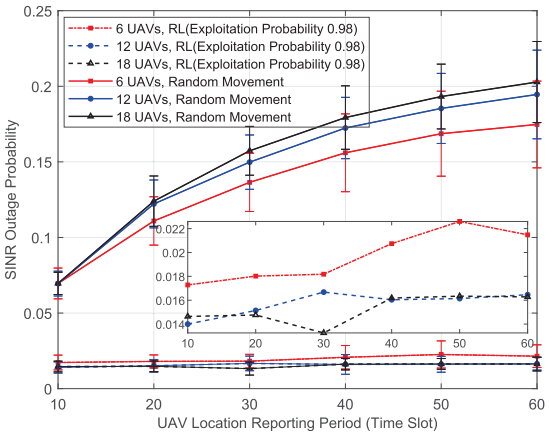

Fig. 11. SINR outage probability vs UAV location reporting period.

the maximum tolerable outage probability 0.05. This verifies the effectiveness of *SwarmShare* in cross-system interference control. It can also be seen that the incumbent network's capacity does not decrease obviously as the number of UAVs increases (e.g., from 12 to 18). This is because, as more UAVs are deployed in a network with fixed number of ground users, some UAVs will not serve any ground users and hence become inactive and cause no interference to the incumbent system.

D. Average Results

In Fig. 9 we report the average capacity achievable by the incumbent system and the UAV network with the number of UAVs varying from 3 to 15 at step of 3. Three UAV mobility patterns are considered: i) random movement;

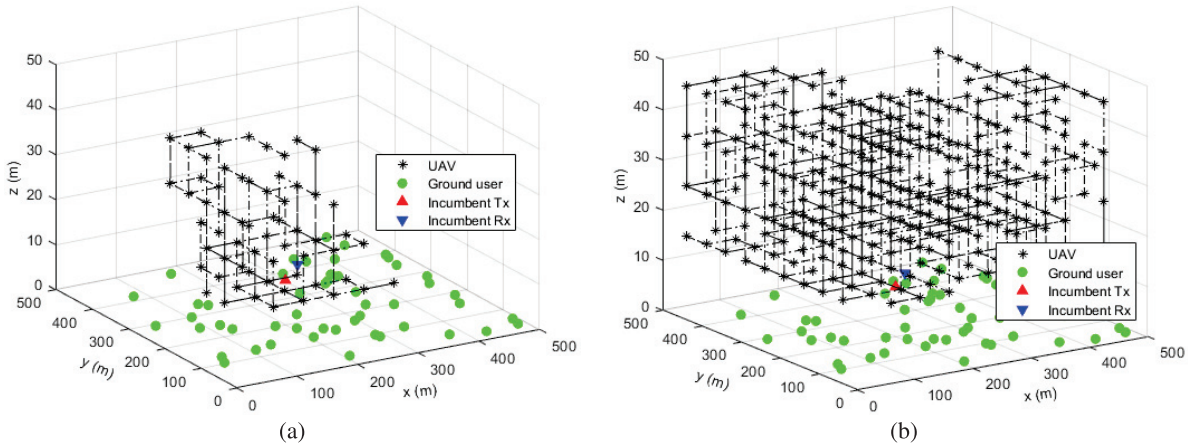

Fig. 12. Example of UAV trajectory with location reporting period of 60 time slots. (a) RL-guided movement; (b) random movement.

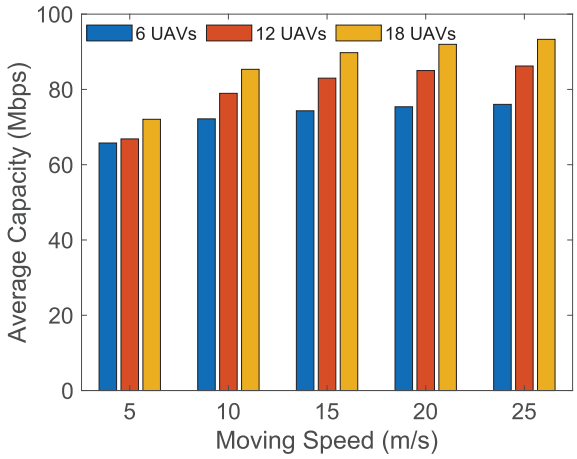

Fig. 13. Average UAV network capacity vs. UAV moving speed.

ii) reinforcement learning controlled movement with exploitation probability of 0.98; and iii) hovering UAVs. The results are obtained by averaging over 50000 time slots for each mobility pattern. It can be seen that, as expected, obvious capacity gain can be achieved by the UAV network with all the above three mobility patterns by deploying more UAVs. For example, for hovering UAVs, the average capacity increases from around 60 Mbps with 3 UAVs to 80 Mbps with 15 UAVs. The capacity is further increased to around 100 Mbps with RL-controlled UAV movement. Particularly, we find that there is no obvious degradation in the capacity of the incumbent system when there are 6 or more coexisting UAVs. The average capacity of the incumbent system can be further increased with less UAVs, e.g., 3, because of the reduced cross-system interference.

In Fig. 10, we report the average capacity achievable by the incumbent system and the UAVsunder different violation probability constraints. Two UAV mobility patterns are considered: i) hovering UAVs and ii) moving UAVs guided by reinforcement learning. The exploitation probability is set to 0.98 for the latter case. Similar to Fig. 9, the aggregate capacity of the UAV networks can be increased significantly by deploying more UAVs. For example, 70 Mbps can be achieved with 9 hovering UAVs and violation probability threshold 0.02, which goes up to 76 Mbps with 15 UAVs. The corresponding incumbent user capacity are 55 Mbps and 54 Mbps. It can also be seen that significant capacity gain can be achieved by RL-guided UAV control. For example, 84 Mbps and 94 Mbps can be achieved with 9 and 15 UAVs, which are 1.52 and 1.74 times higher than that with hovering UAVs. Similar results can also be observed with a violation probability threshold 0.05.

In previous experiments (in Fig. 7) the UAVs report their locations to the AFC in every time slot. In this experiment, we investigate the mobility resilience of *SwarmShare* for spectrum sharing in the presence of inaccurate UAV locations. The SINR outage probability results are reported in Fig. 11, where two mobility patterns are considered for the UAVs, i.e., random movement and RL-guided movement, and the maximum tolerable SINR outage probability is set to 0.05 for the incumbent system. The location reporting period is varied from 10 time slots to 60. It can be seen that the SINR outage probability of the incumbent system increases monotonically with the location reporting period if the UAVs move in an uncontrolled manner, i.e., completely randomly. For example, the outage probability is around 0.07 when the reporting period is 10 time slots and can be up to 0.2 for 60 time slots. In the case of controlled UAV movement, the SINR outage probability is barely affected by the location reporting period and always below the maximum tolerable. This is because, as illustrated by the example trajectories in Fig. 12, the UAVs will stick with their current best locations at a high probability (0.98 in this experiment) while exploring new locations at a low probability (0.02). As a result, the topology of the UAV network and hence the statistical behavior of their aggregate interference to the incumbent system changes only slowly. Therefore, with controlled UAV movement, effective interference control can be achieved with *SwarmShare* in mobile scenarios even with inaccurate UAV locations, e.g., because of the temporary loss of the connections to the AFC.

E. Effects of UAV Moving Speed

In this experiment, we study the effects of the UAV moving speed on the throughput achievable by the UAV network.

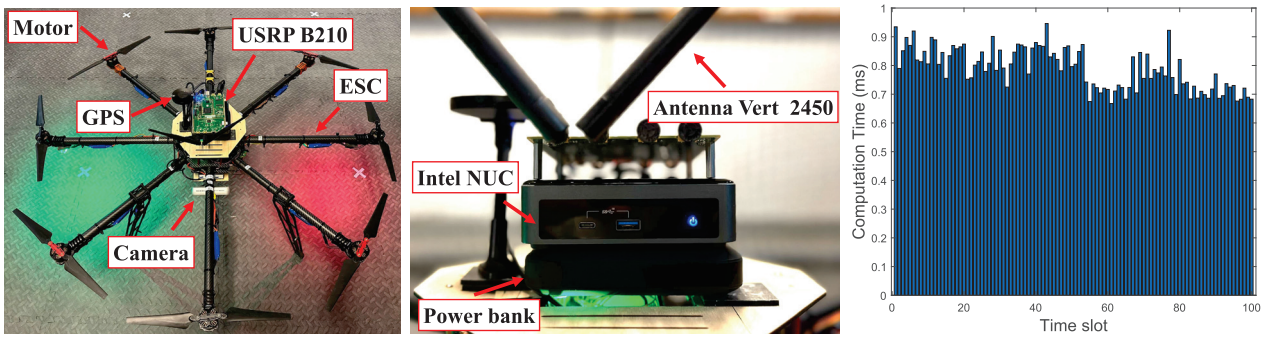

(a) (b) (c)

Fig. 14. (a) Snapshot of octocopter UAV, (b) onboard computing device Intel NUC, and (c) computation time.

Consider 12, 15 and 18 UAVs in the network and the maximum moving speed of UAVs is set to 25 m/s. The duration of each time slot is set to 30 seconds. The results are reported in Fig. 13. It can be seen that, as expected, a larger average throughput can be achieved by the UAV network with higher moving speed. This is because we consider in each time slot that each UAV first moves to the new position before providing service to ground users, and hence with higher moving speed each UAV can arrive at the target position faster and start to serve the ground users sooner.

F. Computational Complexity

We further study the computational time of the UAVs. In this experiment, each UAV needs to finish two tasks in each time slot: transmission power initialization and RL-guided trajectory optimization. For the first task, each UAV calculates its initial power based on three Sigmoid functions defined in (15). In the second task, each UAV determines its next-step movement based on the RL algorithm described in Sec. IV-C. We conduct the experiments on Next Unit of Computing (NUC) with Intel® Core ™ i5-10210U CPU @ 1.60 GHz ×8, memory of 16 GB, and Ubuntu 20.04 Operating System. The dimension of NUC is 117 × 112 × 37 mm^3 and with weight of 504 g. As shown in Figs. 14(a) and (b), NUC has been integrated with the octocopter UAV custom-designed in our lab as the onboard computing device. The results are reported in Fig. 14(c). It can be seen that it takes less than 1 ms for each UAV to finish the two tasks in each step. Since the UAV movement usually operates at a much larger time scale, this verifies the low computational complexity of spectrum sharing algorithm.

VI. Extension to Multiple Incumbent Users

In previous sections, we consider the spectrum coexistence framework between a UAV network and a single incumbent user pair. The framework can also be extended to the scenarios with multiple incumbent user pairs. To this end, we need to further consider the interference among the unpaired incumbent transmitters and receivers, and consider the cross-system interference constraint for each of the incumbent user pairs. Denote $\mathcal{L}$ as the set of the incumbent user pairs and further denote $\gamma^t_{\mathrm{Rx}_l}$ as the SINR of incumbent receiver Rx_l in time slot t. Then the SINR expression in (6) can be rewritten as in (24), shown at the bottom of the page. The SINR for UAV $k \in \mathcal{K}$ can be recalculated similarly. For each incumbent Rx $l \in \mathcal{L}$, a power adaptation coefficient η^t will be calculated following the same procedure as in Sec. IV. In the case that the UAV network is deployed nearby the overlapping area of multiple incumbent user pairs, the smallest η^t will be used for power adaptation for the UAV networks so that the cross-system interference constraints can be satisfied for all the incumbent user pairs. Recall in Sec. IV-D that the power adaptation coefficient η^t can be calculated for each incumbent user pair based on bisection search with almost constant computational complexity. The overall computational complexity in the case of multiple incumbent user pairs is hence $O(|\mathcal{L}|)$, with $|\mathcal{L}|$ representing the number of incumbent user pairs in $\mathcal{L}$.

We further verify the effectiveness of the spectrum coexistence framework considering two and three incumbent user pairs. Consider 6 UAVs moving according to the ϵ-greedy RL algorithm with exploration probability 0.02. The results are reported in Fig. 15 for two incumbent user pairs. Incumbent transmitters (Tx_0 and Tx_1) and receivers (Rx_0 and Rx_1) are deployed with coordinates (120, 250, 10), (380, 250, 10), (50, 250, 10) and (450, 250, 10), respectively. The threshold of violation probability is set to 5% for each incumbent receiver. It can be seen that the violation probability is lower than the threshold for both incumbent user pairs, which are 0.6% and 0.7% for incumbent receiver Rx_0 and Rx_1, respectively. Similar results can also be obtained for three incumbent user pairs.

$$\gamma^t_{\mathrm{Rx}_l} = \frac{p_{\mathrm{Tx}_l} w^{\max}_{\mathrm{Tx}_l} w^{\max}_{\mathrm{Rx}_l} \cdot (h^t_{\mathrm{Tx}_l\mathrm{Rx}_l})^2 / H^{\mathrm{LoS}}_{\mathrm{Tx}_l\mathrm{Rx}_l}}{\underbrace{\sum_{k\in\mathcal{K}} p^t_k w^t_{k\mathrm{Rx}_l} w_k \cdot (h^t_{k\mathrm{Rx}_l})^2 / H^t_{k\mathrm{Rx}_l}}_{Interference\ from\ UAVs} + \underbrace{\sum_{j\in\mathcal{L}, j\neq l} p_{\mathrm{Tx}_j} w_{\mathrm{Rx}_l} w_{\mathrm{Tx}_j} \cdot (h^t_{\mathrm{Tx}_j\mathrm{Rx}_l})^2 / H^t_{\mathrm{Tx}_j\mathrm{Rx}_l}}_{Interference\ from\ Unpaired\ Incumbent\ Txs} + \underbrace{(\sigma_{\mathrm{Rx}_l})^2}_{Noise}} \tag{24}$$

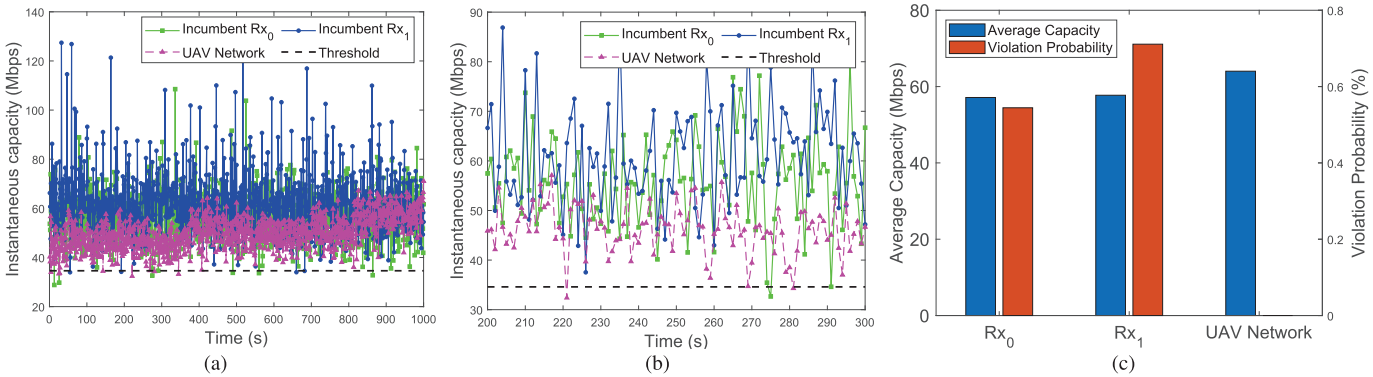

Fig. 15. Spectrum sharing between two incumbent user pairs and 6 UAVs. (a) Instantaneous capacity of the incumbent system and the UAV network; (b) zoomed in plot of time slots 200-300; and (c) average capacity and violation probability.

VII. Conclusion

In this paper, we proposed a new framework called *SwarmShare* to enable spectrum sharing between the incumbent systems and the coexisting UAV networks in the 6 GHz band. We validated the effectiveness of the framework through an extensive simulation campaign. *SwarmShare* is shown to be mobility-resilient and hence is suitable for the operations of moving vehicles such as cars and UAVs on this newly opened spectrum band *without* requiring pre-defined exclusion zones. It is also found that the aggregate interference of the UAVs does not follow any existing distributions. In future work, we will develop new theoretical models to characterize the aggregate interference of the UAVs; reduce the power consumption of the UAV network by jointly optimizing the UAV transmission power and their trajectories under the cross-system interference constraints; enhance spectral efficiency by considering multiple UAVs serving a ground user; and further validate the effectiveness of *SwarmShare* over the UAV testing facilities being developed at University at Buffalo.

Acknowledgment

The contractor acknowledges the Government's support in the publication of this article. Any opinions, findings, and conclusions or recommendations expressed in this material are those of the author(s) and do not necessarily reflect the views of the United States Air Force.

References

[1] J. Hu et al., "SwarmShare: Mobility-resilient spectrum sharing for swarm UAV networking in the 6 GHz band," in *Proc. 18th Annu. IEEE Int. Conf. Sens., Commun., Netw. (SECON)*, Jul. 2021, pp. 1–9.

[2] Z. Chu, W. Hao, P. Xiao, and J. Shi, "UAV assisted spectrum sharing ultra-reliable and low-latency communications," in *Proc. IEEE Global Commun. Conf. (GLOBECOM)*, Waikoloa, HI, USA, Dec. 2019, pp. 1–6.

[3] B. Shang, L. Liu, R. M. Rao, V. Marojevic, and J. H. Reed, "3D spectrum sharing for hybrid D2D and UAV networks," *IEEE Trans. Commun.*, vol. 68, no. 9, pp. 5375–5389, Sep. 2020.

[4] Z. Liu, G. Huang, Q. Zhong, H. Zheng, and S. Zhao, "UAV-aided vehicular communication design with vehicle trajectory's prediction," *IEEE Wireless Commun. Lett.*, vol. 10, no. 6, pp. 1212–1216, Jun. 2021.

[5] Z. Wang, L. Duan, and R. Zhang, "Adaptive deployment for UAV-aided communication networks," *IEEE Trans. Wireless Commun.*, vol. 18, no. 9, pp. 4531–4543, Sep. 2019.

[6] T. Do-Duy, L. D. Nguyen, T. Q. Duong, S. R. Khosravirad, and H. Claussen, "Joint optimisation of real-time deployment and resource allocation for UAV-aided disaster emergency communications," *IEEE J. Sel. Areas Commun.*, vol. 39, no. 11, pp. 3411–3424, Nov. 2021.

[7] *Unlicensed Use of 6 GHz Band*, document GN Docket no. 17-183, Oct. 2018.

[8] V. Sathya, S. M. Kala, M. I. Rochman, M. Ghosh, and S. Roy, "Standardization advances for cellular and Wi-Fi coexistence in the unlicensed 5 and 6 GHz bands," *GetMobile, Mobile Comput. Commun.*, vol. 24, no. 1, pp. 5–15, Aug. 2020.

[9] B. Wang, Y. Sun, Z. Sun, L. D. Nguyen, and T. Q. Duong, "UAV-assisted emergency communications in social IoT: A dynamic hypergraph coloring approach," *IEEE Internet Things J.*, vol. 7, no. 8, pp. 7663–7677, Aug. 2020.

[10] J. Lyu, Y. Zeng, and R. Zhang, "Spectrum sharing and cyclical multiple access in UAV-aided cellular offloading," in *Proc. IEEE Global Commun. Conf.*, Singapore, Dec. 2017, pp. 1–6.

[11] H. Wang, J. Wang, G. Ding, J. Chen, Y. Li, and Z. Han, "Spectrum sharing planning for full-duplex UAV relaying systems with underlaid D2D communications," *IEEE J. Sel. Areas Commun.*, vol. 36, no. 9, pp. 1986–1999, Sep. 2018.

[12] T. Q. Duong, L. D. Nguyen, H. D. Tuan, and L. Hanzo, "Learning-aided realtime performance optimisation of cognitive UAV-assisted disaster communication," in *Proc. IEEE Global Commun. Conf. (GLOBECOM)*, Waikoloa, HI, USA, Dec. 2019, pp. 1–6.

[13] B. Ji, Y. Li, D. Cao, C. Li, S. Mumtaz, and D. Wang, "Secrecy performance analysis of UAV assisted relay transmission for cognitive network with energy harvesting," *IEEE Trans. Veh. Technol.*, vol. 69, no. 7, pp. 7404–7415, Jul. 2020.

[14] A. Fotouhi et al., "Survey on UAV cellular communications: Practical aspects, standardization advancements, regulation, and security challenges," *IEEE Commun. Surveys Tuts.*, vol. 21, no. 4, pp. 3417–3442, 4th Quart., 2019.

[15] Z. Ullah, F. Al-Turjman, and L. Mostarda, "Cognition in UAV-aided 5G and beyond communications: A survey," *IEEE Trans. Cognit. Commun. Netw.*, vol. 6, no. 3, pp. 872–891, Sep. 2020.

[16] Y. Zhou, F. Zhou, H. Zhou, D. W. K. Ng, and R. Q. Hu, "Robust trajectory and transmit power optimization for secure UAV-enabled cognitive radio networks," *IEEE Trans. Commun.*, vol. 68, no. 7, pp. 4022–4034, Jul. 2020.

[17] J. Xiang, Y. Zhang, and T. Skeie, "Joint admission and power control for cognitive radio cellular networks," in *Proc. 11th IEEE Singap. Int. Conf. Commun. Syst.*, Guangzhou, China, Nov. 2008, pp. 1519–1523.

[18] H. Guo, R. Long, and Y. Liang, "Cognitive backscatter network: A spectrum sharing paradigm for passive IoT," *IEEE Wireless Commun. Lett.*, vol. 8, no. 5, pp. 1423–1426, Oct. 2019.

[19] P. K. Sangdeh, H. Pirayesh, A. Quadri, and H. Zeng, "A practical spectrum sharing scheme for cognitive radio networks: Design and experiments," *IEEE/ACM Trans. Netw.*, vol. 28, no. 4, pp. 1818–1831, Aug. 2020.

[20] H. Zhang, N. Yang, W. Huangfu, K. Long, and V. C. M. Leung, "Power control based on deep reinforcement learning for spectrum sharing," *IEEE Trans. Wireless Commun.*, vol. 19, no. 6, pp. 4209–4219, Jun. 2020.

[21] L. Li et al., "Accelerating model-free reinforcement learning with imperfect model knowledge in dynamic spectrum access," *IEEE Internet Things J.*, vol. 7, no. 8, pp. 7517–7528, Aug. 2020.

[22] M. Labib, A. F. Martone, V. Marojevic, J. H. Reed, and A. I. Zaghloul, "A stochastic optimization approach for spectrum sharing of radar and LTE systems," *IEEE Access*, vol. 7, pp. 60814–60826, 2019.

[23] C. Aydogdu, M. F. Keskin, N. Garcia, H. Wymeersch, and D. W. Bliss, "RadChat: Spectrum sharing for automotive radar interference mitigation," *IEEE Trans. Intell. Transp. Syst.*, vol. 22, no. 1, pp. 416–429, Jan. 2021.

[24] A. F. Martone, K. A. Gallagher, and K. D. Sherbondy, "Joint radar and communication system optimization for spectrum sharing," in *Proc. IEEE Radar Conf. (RadarConf)*, Boston, MA, USA, Apr. 2019, pp. 1–6.

[25] C. Zhang, C. Jiang, L. Kuang, J. Jin, Y. He, and Z. Han, "Spatial spectrum sharing for satellite and terrestrial communication networks," *IEEE Trans. Aerosp. Electron. Syst.*, vol. 55, no. 3, pp. 1075–1089, Jun. 2019.

[26] M. L. Attiah, A. A. M. Isa, Z. Zakaria, M. K. Abdulhameed, M. K. Mohsen, and I. Ali, "A survey of mmWave user association mechanisms and spectrum sharing approaches: An overview, open issues and challenges, future research trends," *Wireless Netw.*, vol. 26, no. 4, pp. 2487–2514, May 2020.

[27] D. Tarek, A. Benslimane, M. Darwish, and A. M. Kotb, "Survey on spectrum sharing/allocation for cognitive radio networks Internet of Things," *Egyptian Informat. J.*, vol. 21, no. 4, pp. 231–239, Dec. 2020.

[28] J. Ren, Y. He, G. Huang, G. Yu, Y. Cai, and Z. Zhang, "An edge-computing based architecture for mobile augmented reality," *IEEE Netw.*, vol. 33, no. 4, pp. 162–169, Jul. 2019.

[29] J. Cui, Y. Liu, and A. Nallanathan, "Multi-agent reinforcement learning-based resource allocation for UAV networks," *IEEE Trans. Wireless Commun.*, vol. 19, no. 2, pp. 729–743, Feb. 2020.

[30] S. K. Moorthy and Z. Guan, "FlyTera: Echo state learning for joint access and flight control in THz-enabled drone networks," in *Proc. 17th Annu. IEEE Int. Conf. Sens., Commun., Netw. (SECON)*, Como, Italy, Jun. 2020, pp. 1–9.

[31] L. Bertizzolo, E. Demirors, Z. Guan, and T. Melodia, "CoBeam: Beamforming-based spectrum sharing with zero cross-technology signaling for 5G wireless networks," in *Proc. IEEE Conf. Comput. Commun.*, Toronto, ON, Canada, Jul. 2020, pp. 1429–1438.

[32] Y. Li, H. Zhang, K. Long, S. Choi, and A. Nallanathan, "Resource allocation for optimizing energy efficiency in NOMA-based fog UAV wireless networks," *IEEE Netw.*, vol. 34, no. 2, pp. 158–163, Mar. 2020.

[33] N. Vervliet, O. Debals, L. Sorber, and L. De Lathauwer, "Breaking the curse of dimensionality using decompositions of incomplete tensors: Tensor-based scientific computing in big data analysis," *IEEE Signal Process. Mag.*, vol. 31, no. 5, pp. 71–79, Sep. 2014.

[34] K. T. Hemachandra and N. C. Beaulieu, "Novel representations for the equicorrelated multivariate non-central chi-square distribution and applications to MIMO systems in correlated Rician fading," *IEEE Trans. Commun.*, vol. 59, no. 9, pp. 2349–2354, Sep. 2011.

[35] S. Kusaladharma and C. Tellambura, "Aggregate interference analysis for underlay cognitive radio networks," *IEEE Wireless Commun. Lett.*, vol. 1, no. 6, pp. 641–644, Dec. 2012.

[36] A. A. Khuwaja, Y. Chen, and G. Zheng, "Effect of user mobility and channel fading on the outage performance of UAV communications," *IEEE Wireless Commun. Lett.*, vol. 9, no. 3, pp. 367–370, Mar. 2020.

[37] A. F. Schmidt and C. Finan, "Linear regression and the normality assumption," *J. Clin. Epidemiol.*, vol. 98, pp. 146–151, Jun. 2018.

[38] S. K. Moorthy and Z. Guan, "Beam learning in mmWave/THz-band drone networks under in-flight mobility uncertainties," *IEEE Trans. Mobile Comput.*, vol. 21, no. 6, pp. 1945–1957, Jun. 2022.

[39] S. A. Al-Ahmed, M. Z. Shakir, and S. A. R. Zaidi, "Optimal 3D UAV base station placement by considering autonomous coverage hole detection, wireless backhaul and user demand," *J. Commun. Netw.*, vol. 22, no. 6, pp. 467–475, Dec. 2020.

[40] R. S. Sutton and A. G. Barto, *Reinforcement Learning: An Introduction*. Cambridge, MA, USA: MIT Press, 2018.

[41] D. W. Hosmer Jr., S. Lemeshow, and R. X. Sturdivant, *Applied Logistic Regression*. Hoboken, NJ, USA: Wiley, 2013.

[42] *SimPy*. Accessed: Apr. 2019. [Online]. Available: https://pypi.org/project/simpy/

[43] Z. Guan, T. Melodia, and G. Scutari, "To transmit or not to transmit? Distributed queueing games in infrastructureless wireless networks," *IEEE/ACM Trans. Netw.*, vol. 24, no. 2, pp. 1153–1166, Apr. 2016.

[44] R. K. Ganti and M. Haenggi, "Interference in ad hoc networks with general motion-invariant node distributions," in *Proc. IEEE Int. Symp. Inf. Theory*, Toronto, ON, Canada, Jul. 2008, pp. 1–5.

Jiangqi Hu (Graduate Student Member, IEEE) received the B.E. degree in telecommunication engineering from Dalian Jiaotong University, Dalian, China, in 2016, and the M.S. degree in telecommunication engineering from Xidian University, Xi'an, China, in 2019. He is currently pursuing the Ph.D. degree with the Department of Electrical Engineering, The State University of New York at Buffalo (SUNY Buffalo), Buffalo, NY, USA. He is also working with the UB WINGS Laboratory under the guidance of Prof. Zhangyu Guan. His current research interests include new spectrum technologies and testbed for future networks.

Sabarish Krishna Moorthy (Student Member, IEEE) received the B.E. degree in electronics and communication engineering from the Velammal Engineering College, Chennai, India, in 2016, and the M.S. degree in electrical engineering from the Department of Electrical Engineering, The State University of New York at Buffalo (SUNY Buffalo), Buffalo, NY, USA, in 2018, where he is currently pursuing the Ph.D. degree. He is also working with the UB WINGS Laboratory under the guidance of Prof. Zhangyu Guan. His current research interests include new spectrum technologies and network design automation.

Ankush Harindranath (Student Member, IEEE) received the B.S. degree in electronics and communication engineering from the Ramaiah institute of technology in 2019 and the M.S. degree in electrical engineering from The State University of New York at Buffalo (SUNY Buffalo), Buffalo, NY, USA, in 2021. He is currently an Engineer with the Modem Systems Test Team, Wireless Research and Development Division, Qualcomm.

Zhaoxi Zhang received the bachelor's degree in measurement control technologies and instruments from Beijing Normal University, Zhuhai, China, in 2020, and the master's degree in electrical engineering from The State University of New York at Buffalo (SUNY Buffalo), Buffalo, NY, USA, in 2023, where he is currently pursuing the Ph.D. degree in electrical engineering. His research interests include large-scale real-time digital twin construction and network simulation.

Zhiyuan Zhao received the B.S. degree in electrical engineering from The State University of New York at Buffalo (SUNY Buffalo), Buffalo, NY, USA, in 2021, where he is currently pursuing the M.S. degree. He is a Senior Research Assistant at SUNY Buffalo. His research interests include autonomous UAVs and software-defined wireless networking.

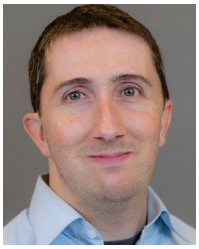

Nicholas Mastronarde (Senior Member, IEEE) received the B.S. and M.S. degrees in electrical engineering from the University of California at Davis, Davis, CA, USA, in 2005 and 2006, respectively, and the Ph.D. degree in electrical engineering from the University of California at Los Angeles, Los Angeles, CA, USA, in 2011. He is currently an Associate Professor with the Department of Electrical Engineering, The State University of New York at Buffalo (SUNY Buffalo), Buffalo, NY, USA. His research interests include reinforcement learning, Markov decision processes, resource allocation and scheduling in wireless networks and systems, UAV networks, and 5G and beyond networks.

Elizabeth Serena Bentley (Member, IEEE) received the B.S. degree in electrical engineering from Cornell University, the M.S. degree in electrical engineering from Lehigh University, and the Ph.D. degree in electrical engineering from The State University of New York at Buffalo. She was a National Research Council Postdoctoral Research Associate with the Air Force Research Laboratory (AFRL), Rome, NY, USA. She is currently employed by the AFRL Information Directorate, where she is performing in-house research and development with the Communication Systems and Technology Branch and managing the "Zero-Day Waveforms for Intelligent and Assured Connectivity (ZoDIAC)" program. Her research interests include cross-layer optimization, swarm networking, directional networking, wireless multiple-access communications, and modeling and simulation.

Scott Pudlewski (Senior Member, IEEE) received the B.S. degree in electrical engineering from the Rochester Institute of Technology, Rochester, NY, USA, in 2008, and the M.S. and Ph.D. degrees in electrical engineering from The State University of New York at Buffalo (SUNY Buffalo), Buffalo, NY, USA, in 2010 and 2012, respectively. He is currently a Senior Research Engineer with the Georgia Tech Research Institute (GTRI), Atlanta, GA, USA. His main research interests include network vulnerabilities, the Internet of Things, networking in contested tactical networks, convex optimization, and wireless networks in general.

Zhangyu Guan (Senior Member, IEEE) received the Ph.D. degree in communication and information systems from Shandong University, China, in 2010. He is currently an Assistant Professor with the Department of Electrical Engineering, The State University of New York at Buffalo, where he directs the Wireless Intelligent Networking and Security (WINGS) Laboratory. His research interests include network design automation, new spectrum technologies, and wireless network security. He has served as the TPC Chair for IEEE INFOCOM Workshop on Wireless Communications and Networking in Extreme Environments (WCNEE) 2020, the Student Travel Grants Chair for IEEE Sensor, Mesh and Ad Hoc Communications and Networks (SECON) from 2019 to 2020, the Information System (EDAS) Chair for IEEE Consumer Communications Networking Conference (CCNC) from 2021 to 2023, the TPC Vice-Chair for IEEE CCNC 2024, and the TPC Chair for IEEE CCNC 2025. He has been serving as an Area Editor for *Journal of Computer Networks* (Elsevier) since July 2019.